Contribution from the Fuzhou Laboratory of Structural Chemistry and Fujian Institute of Research on the Structure of Matter, Chinese Academy of Sciences, Fuzhou, Fujian 350002, China

Structural Chemistry of Molybdenum-Iron-Sulfur Cluster Compounds with a Single-Cubane $[MoFe_3S_4]^{n+}$ (n = 4-6) Core and Crystal Structure of $[MoFe_3S_4(Me_2dtc)_5]\cdot 2CH_2Cl_2$

Qiutian Liu, Liangren Huang, Hanqin Liu,* Xinjian Lei, Daxu Wu, Beisheng Kang, and Jiaxi Lu

Received November 2, 1988

$[MoFe_3S_4(Me_2dtc)_5]\cdot 2CH_2Cl_2$ (A1·$2CH_2Cl_2$) crystallizes in the orthorhombic space group *Pbcn*, with a = 20.335 (13) Å, b = 19.978 (2) Å, c = 10.357 (3) Å, V = 4207.6 Å^3, d_c = 1.835 g/cm^3, and Z = 4. The structure was determined from 1525 reflections ($F_o^2 > 3\sigma(F_o^2)$) and refined by a full-matrix least-squares method to R = 0.074. The complex contains a cubane-like $[MoFe_3S_4]^{5+}$ core. Each of the four dimethyldithiocarbamate ligands chelates to one of the four metal atoms, and the fifth ligand forms a bridge between Mo and one Fe atoms. A series of single-cubane-like clusters with a core structure of $[MFe_3S_4]^{n+}$ (M = Mo, W, n = 4-6; M = Fe, n = 3, 4) were prepared by spontaneous self-assembly reactions or by the conversions of compounds with linear frameworks. The structural parameters of the clusters are compared and discussed. The complexes were characterized by Mössbauer effects, cyclic voltammograms, and ^{1}H NMR techniques. Each Fe atom of oxidation state 3+ interacts magnetically with other metal atoms in the $[MFe_3S_4]^{5+}$ core. The extra electron in the reduced core $[MoFe_3S_4]^{4+}$ is delocalized among four metal atoms.

Introduction

Cluster compounds containing one or two cubane-like core units $[Mo_xFe_{4-x}S_4]$ (x = 0-4) have been widely studied[1-11] in an attempt to simulate the active center of 4Fe-4S proteins (x = 0) or molybdenum-iron proteins and to understand the chemical and physical significance of the clusters. In this laboratory, studies of Mo-Fe-S clusters have been motivated by the simulation of the environment of the metal atoms and the spectroscopic properties of nitrogenases. However, there are many fundamental questions to be answered. What is the mechanism of the synthetic reactions? How does the strong magnetic interaction occur among the paramagnetic metal atoms? What is the synergetic effect among different atoms and groups of atoms within a molecule?

In this paper, the preparation and crystal structure of compound $[MoFe_3S_4(Me_2dtc)_5]\cdot 2CH_2Cl_2$ are described in detail. The formation of the series of single-cubane-like compounds $[MFe_3S_4(R_2dtc)_x]^{n-}$[12] (M = Mo, W, Fe; x = 4, 5, 6; n = 0, 1), their structural data, and spectroscopic properties were summarized and compared with data for relevant compounds. For simplicity, the compounds discussed are given the assigned symbols as shown in Figure 1. Preliminary accounts of the preparations and crystal structures of the cluster compounds A2, A3, A4, B, C, D2, and E have been published.[6]

Experimental Section

Preparation of Compounds. All operations were carried out under a pure dinitrogen atmosphere by using Schlenk techniques. Solvents were dried, distilled, and degassed before use. The compound $C_4H_8dtcNH_4$ was purchased from Tokyo Chemical Industry Co. and used without further purification. Reagents R_2dtcNa (R_2 = Me_2, Et_2, C_5H_{10}) were synthesized by the reaction of R_2NH, NaOH, and CS_2 in water. Anhydrous $FeCl_2$ was purchased from Alfa Division Ventron Co. and used as received. Compounds $(NH_4)_2MoS_4$ and $Fe(R_2dtc)_3$ (R_2 = Me_2, Et_2, C_4H_8, C_5H_{10}) were synthesized by literature methods.[13,14] Compounds $Fe(DMF)_6[(FeCl_2)_2MoS_4]$[15] and $Mg(DMF)_6[Fe_2S_2Cl_4]$[16] were prepared as previously reported. Elemental analyses were performed by the Analytical Chemistry Group of this Institute.

Preparation by Spontaneous Self-Assembly Reaction. $[MoFe_3S_4(Me_2dtc)_5]\cdot 2CH_2Cl_2$ (A1·$2CH_2Cl_2$). A mixture of 4.3 g of Me_2dtcNa (30 mmol), 1.9 g of $FeCl_2$ (15 mmol), and 1.3 g of $(NH_4)_2MoS_4$ (5 mmol) in 60 mL of DMF was stirred at room temperature for 16 h. After filtration, the filtrate was reduced to 35 mL and small portions of CH_3CN were added. The precipitate and inorganic salts formed each time were filtered out until black crystalline A1 began to separate. The black microcrystals formed after leaving the filtrate for several days at 5 °C were collected, washed with CH_3CN, and dried in vacuo, affording 3.2 g (60%) of crude A1·DMF. The crude product contaminated by a small amount of $[MoFe_3S_4(Me_2dtc)_6]$ (B) was recrystallized from CH_2Cl_2/CH_3CN to afford A1·CH_2Cl_2. Anal. Calcd for $C_{16}H_{32}Cl_2Fe_3MoN_5S_{14}$: C, 17.83; H, 2.99; Fe, 15.54; Mo, 8.90; N, 6.50;

* To whom correspondence should be addressed at the Fujian Institute of Research on the Structure of Matter.

(1) (a) Bobrik, M. A.; Hodgson, K. O.; Holm, R. H. *Inorg. Chem.* **1977**, *16*, 1851. (b) Bobrik, M. A.; Laskowski, E. J.; Johnson, R. W.; Gillum, W. O.; Berg, J. M.; Hodgson, K. O.; Holm, R. H. *Inorg. Chem.* **1978**, *17*, 1402. (c) Laskowski, E. J.; Reynolds, J. G.; Frankel, R. B.; Foner, S.; Papaefthymiou, G. C.; Holm, R. H. *J. Am. Chem. Soc.* **1979**, *101*, 6562. (d) Kanatzidis, M. G.; Baenziger, N. C.; Coucouvanis, D.; Simopoulos, A.; Kostikas, A. *J. Am. Chem. Soc.* **1984**, *106*, 4500. (e) Kanatzidis, M. G.; Coucouvanis, D. *Inorg. Chem.* **1984**, *23*, 403.

(2) (a) Christou, G.; Garner, C. D. *J. Chem. Soc., Dalton Trans.* **1980**, 2354. (b) Christou, G.; Mascharak, P. K.; Armstrong, W. H.; Papaefthymiou, G. C.; Frankel, R. B.; Holm, R. H. *J. Am. Chem. Soc.* **1982**, *104*, 2820. (c) Wolff, T. E.; Berg, J. M.; Hodgson, K. O.; Frankel, R. B.; Holm, R. H. *J. Am. Chem. Soc.* **1979**, *101*, 4140.

(3) (a) Wolff, T. E.; Berg, J. M.; Power, P. P.; Hodgson, K. O.; Holm, R. H. *Inorg. Chem.* **1980**, *19*, 430. (b) Wolff, T. E.; Power, P. P.; Frankel, R. B.; Holm, R. H. *J. Am. Chem. Soc.* **1980**, *102*, 4694.

(4) (a) Kang, B. S.; Cai, J. H.; Cheng, C. N.; Lu, J. X. *Acta Chim. Sin. (Chin. Ed.)* **1986**, *44*, 206. (b) Kang, B. S.; Huang, L. R.; Cai, J. H.; Yang, Y.; Lu, J. X. *Acta Chim. Sin. (Chin. Ed.)* **1987**, *45*, 1152. (c) Kang, B. S.; Liu, Q. T.; Huang, L. R.; Wu, D. X.; Cai, J. H.; He, L. J.; Liu, H. Q.; Lu, J. X. *Jiegou Huaxue* **1987**, *6*, 7. (d) Liu, H. Q.; Wu, D. X.; Kang, B. S. *Chin. J. Microwave Radio-Freq. Spectrosc.* **1987**, *4*, 13. (e) Liu, H. Q.; Kang, B. S.; Cai, J. H.; Huang, L. R.; Wu, D. X.; Wang, F.; Guo, Z.; Cong, A. Z.; Lu, J. Z. *Jiegou Huaxue* **1988**, *7*, 171. (f) Kang, B. S.; Liu, H. Q.; Wang, F.; Cheng, W. Z.; Lu, C. Z.; Wang, X. P.; Lu, J. X. *Chin. J. Appl. Chem.* **1988**, *5*, 67.

(5) (a) Armstrong, W. H.; Holm, R. H. *J. Am. Chem. Soc.* **1981**, *103*, 6246. (b) Armstrong, W. H.; Mascharak, P. K.; Holm, R. H. *Inorg. Chem.* **1982**, *21*, 1699. (c) Armstrong, W. H.; Mascharak, P. K.; Holm, R. H. *J. Am. Chem. Soc.* **1982**, *104*, 4373. (d) Mascharak, P. K.; Armstrong, W. H.; Mizobe, Y.; Holm, R. H. *J. Am. Chem. Soc.* **1983**, *105*, 475. (e) Mascharak, P. K.; Papaefthymiou, G. C.; Armstrong, W. H.; Foner, S.; Frankel, R. B.; Holm, R. H. *Inorg. Chem.* **1983**, *22*, 2851. (f) Palermo, R. E.; Holm, R. H. *J. Am. Chem. Soc.* **1983**, *105*, 4310. (g) Palermo, R. E.; Singh, R.; Bashkin, J. K.; Holm, R. H. *J. Am. Chem. Soc.* **1984**, *106*, 2600. (h) Zhang, Y. P.; Bashkin, J. K.; Holm, R. H. *Inorg. Chem.* **1987**, *26*, 694.

(6) (a) Liu, Q. T.; Huang, L. R.; Kang, B. S.; Liu, C. W.; Wang, L. L.; Lu, J. X. *Acta Chim. Sin. (Chin. Ed.)* **1986**, *44*, 343. (b) Liu, Q. T.; Huang, L. R.; Kang, B. S.; Yang, Y.; Lu, J. X. *Acta Chim. Sin. (Chin. Ed.)* **1987**, *45*, 133. (c) Liu, Q. T.; Huang, L. R.; Yang, Y.; Lu, J. X. *Acta Chim. Sin. (Chin. Ed.)* **1988**, *46*, 1. (d) Liu, Q. T.; Huang, L. R.; Yang, Y.; Lu, J. X. *Acta Chim. Sin. (Chin. Ed.)* **1988**, *46*, 1075. (e) Liu, Q. T.; Huang, L. R.; Yang, Y.; Lu, J. X. *Kexue Tongbao* **1988**, *33*, 1633. (f) Liu, Q. T.; Huang, L. R.; Yang, Y.; Lu, J. X. *Jiegou Huaxue* **1987**, *6*, 135. (g) Liu, Q. T. Unpublished work. (h) Liu, Q. T.; Kang, B. S.; Cheng, C. N.; Huang, L. R.; Cai, J. H.; Zhuang, B. T.; Lu, J. X. *Sci. Sin., Ser. B: (Chin. Ed.)* **1988**, 920.

(7) Holm, R. H.; Simhon, E. D. In *Molybdenum Enzymes*; Spiro, T. G., Ed.; Wiley Interscience: New York, 1985; Chapter 1.

(8) (a) Kanatzidis, M. G.; Coucouvanis, D.; Simopoulos, A.; Kostikas, A.; Papaefthymiou, V. *J. Am. Chem. Soc.* **1985**, *107*, 4925. (b) Coucouvanis, D.; Challen, P. R.; Koo, S.-M.; Davis, W. M.; Butler, W.; Dunham, W. R. *Inorg. Chem.* **1989**, *28*, 4181.

(9) Brunner, H.; Kanermann, H.; Watchter, J. *Angew. Chem., Int. Ed. Engl.* **1983**, *22*, 549.

(10) Shibahara, T.; Akashi, H.; Kuroya, H. *J. Am. Chem. Soc.* **1986**, *108*, 1342.

0020-1669/90/1329-4131$02.50/0

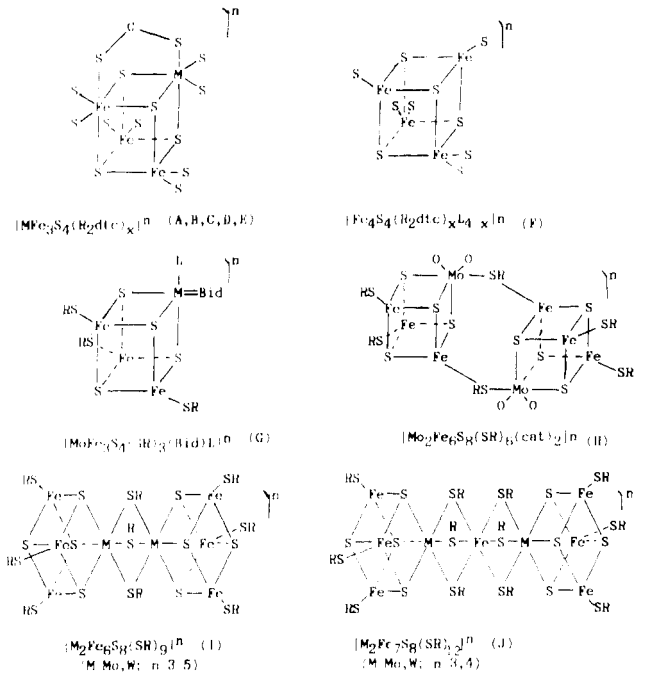

Figure 1. Schematic views for single- and double-cubane anions. Symbol designations of A, B, C, D, E, and F are shown in Figure 3. Bid stands for a bidentate ligand,[5h] and L stands for a monodentate ligand.

S, 41.64. Found: C, 17.42; H, 3.13; Fe, 15.37; Mo, 8.70; N, 6.66; S, 41.47.

$[MoFe_3S_4(Et_2dtc)_5]$·DMF (A2·DMF). The procedure in the preceding preparation was utilized in the synthesis of this compound with of Et_2dtcNa (5.14 g, 30 mmol) used instead of Me_2dtcNa. The black crystalline A2·DMF (2.05 g, 34%) obtained from DMF/CH_3CN was collected, washed with CH_3CN, and dried in vacuo. Anal. Calcd for $C_{28}H_{57}Fe_3MoN_6OS_{14}$: C, 27.88; H, 4.76; Fe, 13.89; Mo, 7.95; N, 6.97; S, 37.21. Found: C, 26.40; H, 4.50; Fe, 13.65; Mo, 7.10; N, 6.65; S, 36.52.

$[MoFe_3S_4(C_5H_{10}dtc)_5]$·DMF (A4·DMF). The procedure in the preceding preparation was utilized in the synthesis of this compound with the use of C_5H_{10}dtcNa (5.5 g, 30 mmol). The black microcrystals (1.8 g, 28%) of A4·DMF separated from DMF/C_6H_6 were collected, washed with benzene, and dried in vacuo. Anal. Calcd for $C_{33}H_{57}Fe_3MoN_6OS_{14}$: C, 31.30; H, 4.54; Fe, 13.23; Mo, 7.58; N, 6.64. Found: C, 31.54; H, 4.64; Fe, 12.62; Mo, 7.69; N, 6.48.

$[WFe_3S_4(Me_2dtc)_5]$ (A5). This compound was obtained by the same procedure as in the preceding preparation with use of $(NH_4)_2WS_4$ and Me_2dtcNa.

$[WFe_3S_4(C_4H_8dtc)_5]$·2DMF (A6·2DMF). A mixture of C_4H_8dtcNH$_4$ (4.9 g, 30 mmol), $(NH_4)_2WS_4$ (1.7 g, 5 mmol), and $FeCl_2$ (1.9 g, 15 mmol) in 80 mL of DMF was stirred for 20 h at room temperature. After filtration, 60 mL of CH_3CN was added to the filtrate. The black precipitate and inorganic salts that separated were filtered off and 40 mL of CH_3CN was added to the filtrate again. After the filtrate was allowed to stand for several days, the black prism-like crystals were collected, washed with acetonitrile, and dried in vacuo to afford 2.0 g (29%) of A6·2DMF. Anal. Calcd for $C_{31}H_{54}Fe_3N_7O_2S_{14}W$: C, 27.44; H, 4.01; Fe, 12.35; N, 7.23; S, 33.08; W, 13.55. Found: C, 27.77; H, 3.98; Fe, 12.42; N, 7.27; S, 32.73; W, 14.00.

$[MoFe_3S_4(Me_2dtc)_6]$·CH_2Cl_2 (B·CH_2Cl_2). Compound B was isolated from the recrystallization solution of A1·DMF (1.5 g) in the mixed solvent CH_2Cl_2/CH_3CN as B·CH_2Cl_2 (0.16 g). Anal. Calcd for $C_{19}H_{38}Cl_2Fe_3MoN_6S_{16}$: C, 19.05; H, 3.20; Fe, 13.99; Mo, 8.01; N, 7.01; S, 42.82. Found: C, 18.69; H, 3.22; Fe, 14.71; Mo, 8.11; N, 7.88; S, 42.71.

$(Et_4N)[MoFe_3S_4(Et_2dtc)_5]$·$CH_3CN$ (C·CH_3CN). A suspension of 7.7 g (45 mmol) of Et_2dtcNa, 1.9 g (15 mmol) of $FeCl_2$, and 3.2 g (15 mmol) of Et_4NBr in 100 mL of DMF was stirred for 2 h and 1.3 g (5 mmol) of $(NH_4)_2MoS_4$ in 15 mL of DMF was added. After being stirred for a further 16 h at room temperature, the solution was filtered and reduced in volume to 40 mL. This concentrated solution was allowed to stand overnight and filtered to remove inorganic salts and some unidentified black precipitates. Acetonitrile was added in portions to the filtrate until the formation of black platelike crystals, which were collected, washed with CH_3CN, and dried in vacuo to afford 2.4 g (37%) of C·CH_3CN. Anal. Calcd for $C_{35}H_{73}Fe_3MoN_7S_{14}$: C, 32.22; H, 5.64; Fe, 12.84; Mo, 7.35; N, 7.51; S, 34.41. Found: C, 33.05; H, 5.58; Fe, 13.05; Mo, 7.01; N, 7.20; S, 35.14.

Preparation by the Conversion of Framework from Linear to Cubic. $[MoFe_3S_4(Et_2dtc)_5]$·DMF (A2·DMF). Compounds $Fe(DMF)_6[(FeCl_2)_2MoS_4]$ (1.0 g, 1.03 mmol) and Et_2dtcNa (1.06 g, 6.18 mmol) were mixed in 25 mL of DMF and stirred for 6–8 h at room temperature. The solution was filtered and reduced in volume to 15 mL. After being cooled at 5 °C overnight, the filtrate was added to 30 mL of CH_3CN after separation of the deposited inorganic salts. After it was left standing at room temperature for several days, the solution gave black square crystals, which were collected, washed with CH_3CN, and dried in vacuo to afford 0.5 g (40%) of A2·DMF. Anal. Calcd for $C_{28}H_{57}Fe_3MoN_6OS_{14}$: C, 27.88; H, 4.76; Fe, 13.89; Mo, 7.95; N, 6.97; S, 37.21. Found: C, 27.74; H, 4.56; Fe, 13.47; Mo, 7.71; N, 7.08; S, 36.52.

$[MoFe_3S_4(C_4H_8dtc)_5]$·CH_2Cl_2 (A3·CH_2Cl_2). The mixture of $Fe(DMF)_6[(FeCl_2)_2MoS_4]$ (0.97 g, 1 mmol) and C_4H_8dtcNH$_4$ (0.98 g, 6 mmol) in 50 mL of DMF was stirred for 8 h at room temperature and filtered, and the filtrate was reduced in volume to 30 mL. The solution was added to 30 mL of benzene and the resulting mixture allowed to stand at 5 °C overnight to afford 1.0 g of crude microcrystalline A3·DMF. This crude product was recrystallized from CH_2Cl_2/CH_3CN to give 0.5 g (41%) of black pyramidal crystals of A3·CH_2Cl_2. Anal. Calcd for $C_{26}H_{42}Cl_2Fe_3MoN_5S_{14}$: C, 25.85; H, 3.50; Cl, 5.87; Fe, 13.87; Mo, 7.94; N, 5.80; S, 37.15. Found: C, 25.50; H, 3.25; Cl, 4.92; Fe, 13.97; Mo, 7.82; N, 5.97; S, 37.00.

$[MoFe_3S_4(C_5H_{10}dtc)_5]$·$^3/_2CH_2Cl_2$ (A4·$^3/_2CH_2Cl_2$). Cluster A4 was prepared by the same procedure as for A3 with the use of C_5H_{10}dtcNa (1.1 g, 6 mmol) instead of C_4H_8dtcNH$_4$. Black platelike crystals of A4·$^3/_2(CH_2Cl_2)$ (0.8 g, 60%) were obtained by recrystallizing the crude product A4·DMF in CH_2Cl_2/CH_3CN. Anal. Calcd for $C_{31.5}H_{53}Cl_3Fe_3MoN_5S_{14}$: C, 28.65; H, 4.05; Cl, 8.05; Fe, 12.69; Mo, 7.26; N, 5.30; S, 33.99. Found: C, 27.99; H, 3.95; Cl, 8.51; Fe, 12.47; Mo, 7.16; N, 5.51; S, 33.78.

$[Fe_4S_4(Et_2dtc)_4]$ (D1). The mixture of $Mg(DMF)_6[Fe_2S_2Cl_4]$ (0.7 g, 0.9 mmol) and Et_2dtcNa (0.34 g, 2 mmol) in 50 mL of CH_2Cl_2 was stirred for 3 h at room temperature and filtered. The filtrate was added to 60 mL of THF and the resulting mixture allowed to stand at 5 °C overnight. The black crystals thus formed were collected and dried in vacuo to afford 0.2 g (48%) of D1. Anal. Calcd for $C_{20}H_{40}Fe_4N_4S_{12}$: C, 25.43; H, 4.27; Fe, 23.65; N, 5.93; S, 40.72. Found: C, 25.69; H, 4.33; Fe, 23.68; N, 6.35; S, 39.17.

The syntheses of $[Fe_4S_4(C_5H_{10}dtc)_4]$ (D2)[6e] and $(Et_4N)[Fe_4S_4(Et_2dtc)_4]$ (E)[6f] were performed according to literature methods.

Collection and Reduction of X-ray Diffraction Data. A single crystal of $[MoFe_3S_4(Me_2dtc)_5]\cdot 2CH_2Cl_2$ (A1·$2CH_2Cl_2$) suitable for diffraction experiment was obtained from slow cooling of a saturated solution of A1·DMF or A1·CH_2Cl_2 in CH_2Cl_2. A black rhombic single crystal was coated with epoxy resin and mounted on a glass fiber. Data collections

Table I. Crystallographic Data and Data Collection Parameters for $[MoFe_3S_4(Me_2dtc)_5]\cdot 2CH_2Cl_2$

formula	$C_{17}H_{34}Cl_4Fe_3MoN_5S_{14}$	fw	1162.68
a, Å	20.335 (13)	space group	*Pbcn* (No. 60)
b, Å	19.978 (2)	temp, °C	23
c, Å	10.357 (3)	radiation used	Mo Kα (0.71069 Å)
V, Å^3	4207.6	d_{calc}, g/cm^3	1.835
Z	4	μ, cm^{-1}	22.48
R	0.074	R_w	0.075

(11) (a) Mak, T. C. W.; Jasim, K. S.; Chieh, C. *Inorg. Chem.* **1985**, *24*, 1587. (b) Bandy, J. A.; Davies, C. E.; Green, J. C.; Green, M. L. H.; Prout, K.; Rodgers, D. P. S. *J. Chem. Soc., Chem. Commun.* **1983**, 1395. (c) Müller, A.; Eltzner, W.; Bögge, H.; Jostes, R. *Angew. Chem., Int. Ed. Engl.* **1982**, *21*, 795. (d) Müller, A.; Eltzner, W.; Clegg, W.; Sheldrick, G. M. *Angew. Chem., Int. Ed., Engl.* **1982**, *21*, 536. (e) Shibahara, T.; Kuroya, H.; Matsumoto, K.; Ooi, S. *J. Am. Chem. Soc.* **1984**, *106*, 789.

(12) Abbreviation: R_2dtc, dialkyldithiocarbamato (R_2NCSS); S_c and S_t, sulfur atoms at core and terminal, respectively; cat, catecholate; C_4H_8, $-(CH_2)_4-$; C_5H_{10}, $-(CH_2)_5-$; dmpe, 1,2-bis(dimethylphosphino)ethane.

(13) (a) Kruss, G. *Justus Liebigs Ann. Chem.* **1884**, *225*, 1. (b) McDonald, J. W.; Friesen, G. D.; Rosenhein, L. D.; Newton, W. E. *Inorg. Chim. Acta* **1981**, *72*, 205.

(14) (a) Cambi, L.; Cagnasso, A. *Atti Accad. Naz. Lincei* **1931**, *13*, 809. (b) Ewald, A. H.; Martin, R. L.; Sinn, E.; White, A. H. *Inorg. Chem.* **1969**, *8*, 1837.

(15) Liu, Q. T.; Huang, L. R.; Kang, B. S.; Lu, J. X. *Jiegou Huaxue* **1983**, *2*, 225.

(16) Huang, L. R.; et al. Unpublished work. $Mg(DMF)_6[Fe_2S_2Cl_4]$ was prepared from the reaction of $MgCl_2$, $FeCl_3$, with NaSH in DMF solution.

were performed at ambient temperature on a Rigaku AFC5R four-circle diffractometer by using Mo Kα radiation and a graphite monochromator. Crystal and data collection parameters are summarized in Table I. The orientation matrices and unit cell parameters were derived from a least-squares fit of 20 machine-centered reflections with 2θ values between 18 and 21°. The three check reflections, monitored periodically during data collection, showed a small fluctuation (0.872–1.031), and the intensity data were scaled accordingly. The data were then corrected for the Lorentz and polarization effects with the program MSC/AFC and for secondary extinction.[17] Systematic absences of $0kl$ ($k \neq 2n$), $h0l$ ($l \neq 2n$), and $hk0$ ($h + k \neq 2n$) uniquely determined the space group as Pbcn.

Structure Solution and Refinement. Calculations were performed on a VAX-11/785 computer with the SDP/VAX package.[18] The structure was first solved by direct methods, and the remaining non-hydrogen atoms were then located by different Fourier syntheses. The asymmetric unit for this initial model is centered at the crystallographic 2-fold axis of the space group, *Pbcn*, such that there is a 2-fold disorder involving atoms Mo and Fe. Therefore, the least-squares refinement of A1·$2CH_2Cl_2$ is performed with a unit containing 0.5 of the cluster molecule and one solvent molecule such that the scattering factor of M is an average of 0.5Mo + 0.5Fe. In order to test the correctness of this disorder model, isotropic refinements were performed by using a lower symmetry space group, $Pca2_1$, for the asymmetric unit A1·$2CH_2Cl_2$, and this resulted in $R = 0.15$ with unacceptable thermal parameters for Mo and Fe atoms of 6.5 and 2.4 Å^2, respectively. Hydrogen atoms were not included in the calculations. Full-matrix least-squares refinements minimized the function $\sum w_i(|F_o| - |F_c|)^2$, and the weight w is defined by Killean's method with terms of $p = 0.010$ and $q = 2.0$.[19]

Atomic scattering factors were taken from ref 20. Anomalous dispersion effects were included in F_c.[21] A total of 1525 reflections with $I > 3\sigma(I)$ were used for the refinements. Isotropic refinements of all the non-hydrogen atoms converged to a R value of 0.129. At this point, an absorption correction using the program DIFABS[22] was applied, and anisotropic refinements of all the non-hydrogen atoms were carried out. The final cycle of refinement included 201 variable parameters and converged (the largest parameter shift was 0.25 time of its esd) with unweighted and weighted agreement factors of

$$R = \sum|F_o - F_c|/\sum|F_o| = 0.074$$

$$R_w = [\sum(F_o - F_c)^2/\sum wF_o^2]^{1/2} = 0.075$$

The standard deviation of an observation with unit weight was 1.77. The maximum and minimum values of e/Å^3 in the final difference Fourier map are 0.72 (18) and −0.78 (17), respectively.

Other Physical Measurements. All measurements were performed under anaerobic conditions. ^{1}H NMR spectra were recorded on a Varian FT-80A or a Varian XL-200 spectrometer with Me_4Si as internal standard. Chemical shifts are reported in ppm, with a positive sign for a resonance appearing downfield from Me_4Si as a general convention. Mössbauer spectra were measured at liquid-nitrogen and room temperatures with a constant-acceleration spectrometer. The source was 50 mCi of cobalt-57 in a Pd matrix and was held at room temperature. Parameters were calibrated with natural-abundance-iron foil at room-temperature. The cyclic voltammeter consisted of a DHZ-1 electrochemical multipurpose instrument and an X-Y recorder. The cyclic voltammogram was performed in a trielectrode cell containing a Pt auxiliary electrode, a SCE reference electrode, and a Pt working electrode and in CH_2Cl_2 solution with $(Bu_4N)BF_4$ as the supporting electrolyte.

Results and Discussion

Syntheses. Cluster compounds containing the cubane-like $[Mo(W)Fe_3S_4]$ unit have been explored at length.[2-6] A series of double-cubane cluster compounds was obtained from the spontaneous self-assembly reaction of simple inorganic salts with monodentate thiolato ligands. However, the self-assembly reaction behaved quite differently when the bidentate ligand R_2dtc was used. First, cluster compounds A, B, and C, containing the single-cubane core $MoFe_3S_4$, were obtained in one-pot reactions, whereas the single-cubane analogues with monodentate thiolates were accessible only through cleavage reactions of the double-cubane cluster $[Mo_2Fe_7S_8(SEt)_{12}]^{3-}$ by bidentate reagent such as catechols or dmpe.[5h] Second, in comparison with single-cubane clusters containing monodentate thiolates, clusters A, B, and C containing R_2dtc have higher oxidation states for the $MoFe_3S_4$ core. The R_2dtc ligands exhibit two coordination modes: chelating to a single metal atom or bridging two metal atoms to satisfy the six-coordination environment of Mo atom. Consequently, the R_2dtc ligand can impel the assembly reaction to form a single-cubane $MoFe_3S_4$ cluster, in which a six-coordinated environment of Mo is required for stability.

The high core oxidation level in clusters A, B, or C can be attributed to the resonance form

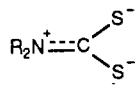

of R_2dtc and to the lower reducing ability of R_2dtc than that of thiolate. The electron-rich S atoms in

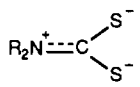

favor the chelation of metal atoms in high oxidation states (vide infra) to increase the stability of the cluster thus formed. Consequently, the core oxidation states of clusters A–E with ligands R_2dtc are higher (A, $[MoFe_3S_4]^{5+}$; B, $[MoFe_3S_4]^{6+}$; C, $[MoFe_3S_4]^{4+}$; D, $[Fe_4S_4]^{4+}$; E, $[Fe_4S_4]^{3+}$) than those of the corresponding clusters with monodentate thiolates[1,5] ($[MoFe_3S_4]^{3+,2+}$ and $[Fe_4S_4]^{2+,+}$). The argument that R_2dtc can stabilize a high oxidation state of the metal atom in $M(Et_2dtc)_n$ has been proposed by Coucouvanis.[1d] Cluster A can also be synthesized by conversion of a linear trimetal compound $Fe(DMF)_6[(FeCl_2)_2MoS_4]$ in the presence of R_2dtc salts.

$$Fe(DMF)_6[(FeCl_2)_2MoS_4] \xrightarrow{R_2dtcNa} [MoFe_3S_4(R_2dtc)_5] \quad (1)$$

$$R_2 = Et_2,\ C_4H_8,\ C_5H_{10}$$

Cluster D was prepared by the combination of two Fe_2S_2 units.

$$2[Mg(DMF)_6][Fe_2S_2Cl_4] \xrightarrow{R_2dtcNa} [Fe_4S_4(R_2dtc)_4] \quad (2)$$

$$R_2 = Et_2,\ C_5H_{10}$$

Both reactions suggest that the spontaneous self-assembly of a single-cubane compound in a system of simple inorganic reactants may pass through a linear oligonuclear intermediate. The latter exists temporarily in the assembly system and is converted into the cubane cluster by chelation of R_2dtc. It is interesting that the conversion of a compound of linear framework to a cubic one was also observed in the reaction of $Fe(DMF)_6[(FeCl_2)_2MoS_4]$ with thiolates.[6c,h] In contrast to the reactions with R_2dtc, which lead to single cubanes, reactions with monodentate thiolates lead to double-cubane clusters.[6h]

$$[(FeCl_2)_2MoS_4]^{2-} \xrightarrow{PhSNa,\ Et_4NBr} (Et_4N)_3[Mo_2Fe_6S_8(SPh)_9] \quad (3)$$

Equations 1 and 3 demonstrate that the dialkyldithiocarbamato ligand plays an important role in forming the single-cubane core $MoFe_3S_4$ or Fe_4S_4 with a high oxidation level.

Crystallographic Studies. Description of the Structure of $[MoFe_3S_4(Me_2dtc)_5]\cdot 2CH_2Cl_2$ (A1·$2CH_2Cl_2$). The crystal structure of A1·$2CH_2Cl_2$ consists of four cluster molecules and eight solvate CH_2Cl_2 molecules in an unit cell. Positional parameters of the non-hydrogen atoms are listed in Table II. The cluster structure is depicted in Figure 2. Selected interatomic distances and bond angles are collected in Tables III and IV, respectively. The solvate molecules have unexceptional structures and will not be considered further.

The innermost core of the cluster is a tetrahedral $MoFe_3$ unit. Each face of the tetrahedron is capped with a sulfur atom that bridges three metal atoms. The final "cubane" possesses a 2-fold

(17) Zachariasen, W. H. *Acta Crystallogr.* **1963**, *16*, 1139.
(18) Frenz, B. A. In *Computing in Crystallography*; Schenk, H., Olthof-Hazekamp, R., Van Koningsveld, H., Bassi, G. C., Eds.; Delft University Press: Delft, The Netherlands, 1978. Modified by L. R. Huang.
(19) Killean, R. C. G.; Lawrence, J. L. *Acta Crystallogr.* **1969**, *B25*, 1750.
(20) Cromer, D. T.; Waber, J. T. In *International Tables for X-ray Crystallography*; Ibers, J. A., Hamilton, W. C., Eds.; The Kynoch Press: Birmingham, England, 1974; Vol. IV, p 71.
(21) Ibers, J. A.; Hamilton, W. C. *Acta Crystallogr.* **1964**, *17*, 781.
(22) Walker, N.; Stuart, D. *Acta Crystallogr.* **1983**, *A39*, 158.

Table II. Positional Parameters for $[MoFe_3S_4(Me_2dtc)_5]\cdot 2CH_2Cl_2$

atom	x	y	z	B_{eqv},[a] Å^2
M	0.55155 (9)	0.1950 (1)	0.1685 (2)	3.53 (4)
Fe	0.4654 (1)	0.3003 (2)	0.1368 (2)	3.03 (5)
S(1)	0.5732 (2)	0.3058 (3)	0.1655 (5)	3.7 (1)
S(2)	0.4446 (2)	0.1912 (3)	0.1154 (4)	3.4 (1)
S(11)	0.6717 (2)	0.1796 (3)	0.1490 (5)	3.5 (1)
S(12)	0.5818 (2)	0.1908 (3)	-0.0594 (4)	3.1 (1)
S(13)	0.5570 (3)	0.0721 (2)	0.1529 (5)	3.4 (1)
S(21)	0.4463 (3)	0.3079 (3)	-0.0801 (5)	4.4 (1)
S(22)	0.4394 (3)	0.4119 (3)	0.1000 (5)	4.5 (1)
N(1)	0.7112 (6)	0.1938 (8)	-0.096 (1)	3.5 (3)
N(2)	0.4028 (9)	0.4299 (8)	-0.149 (2)	5.0 (4)
N(3)	0.5000	-0.034 (1)	0.2500	2.5 (4)
C(10)	0.6620 (7)	0.188 (1)	-0.013 (2)	3.2 (4)
C(11)	0.7826 (8)	0.190 (1)	-0.052 (2)	4.8 (5)
C(12)	0.696 (1)	0.198 (1)	-0.239 (2)	5.1 (5)
C(20)	0.4289 (8)	0.391 (1)	-0.060 (2)	3.8 (5)
C(21)	0.386 (1)	0.500 (1)	-0.115 (2)	6.3 (6)
C(22)	0.399 (1)	0.408 (1)	-0.282 (2)	6.2 (6)
C(30)	0.5000	0.034 (1)	0.2500	2.6 (6)
C(31)	0.4547 (8)	-0.0694 (9)	0.336 (2)	3.4 (4)
C	0.683 (1)	0.035 (2)	0.413 (3)	5.2 (7)
Cl(1)	0.7262 (6)	0.1016 (5)	0.4752 (9)	9.1 (3)
Cl(2)	0.7232 (5)	-0.0185 (5)	0.334 (1)	10.5 (4)

[a] Values for anisotropically refined atoms are given in the form of the isotropic equivalent displacement parameter defined as (4/3) $[a^2B_{11} + b^2B_{22} + c^2B_{33} + ab(\cos\gamma)B_{12} + ac(\cos\beta)B_{13} + bc(\cos\alpha)B_{23}]$

Table III. Selected Interatomic Distances (Å) for $[MoFe_3S_4(Me_2dtc)_5]\cdot 2CH_2Cl_2$

M-M′	2.692 (4)	S(11)-C(10)	1.61 (1)
M-Fe	2.758 (3)	S(12)-C(10)	1.71 (1)
M-Fe′	2.937 (3)	S(13)-C(30)	1.72 (1)
Fe-Fe′	2.737 (4)	S(21)-C(20)	1.73 (2)
M-S(1)	2.260 (5)	S(22)-C(20)	1.73 (2)
M-S(2)	2.242 (4)	N(1)-C(10)	1.32 (2)
M-S(2)′	2.241 (5)	N(1)-C(11)	1.51 (2)
Fe-S(1)	2.221 (4)	N(1)-C(12)	1.50 (2)
Fe-S(1)′	2.200 (5)	N(2)-C(20)	1.30 (2)
Fe-S(2)	2.236 (5)	N(2)-C(21)	1.49 (3)
M-S(11)	2.471 (4)	N(2)-C(22)	1.45 (2)
M-S(12)	2.441 (4)	N(3)-C(30)	1.37 (3)
M-S(13)	2.458 (5)	N(3)-C(31)	1.46 (2)
Fe-S(21)	2.284 (4)	C-Cl(1)	1.76 (3)
Fe-S(22)	2.326 (6)	C-Cl(2)	1.58 (3)

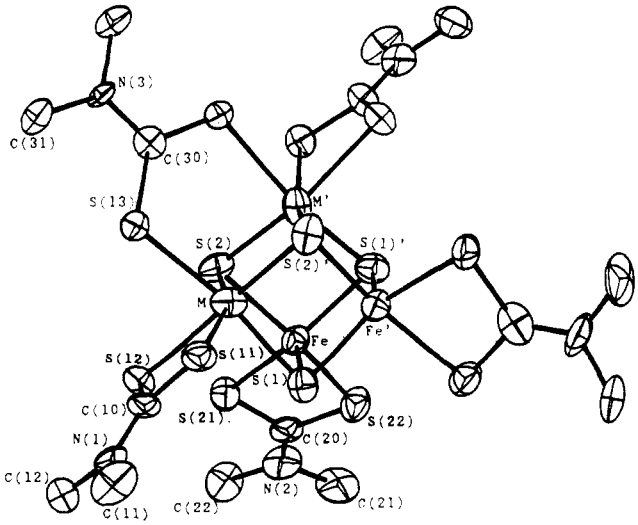

Figure 2. Structure of $[MoFe_3S_4(Me_2dtc)_5]$ with the numbering scheme for the non-hydrogen atoms and the 50% probability ellipsoids.

axis through atoms C(30) and N(3). The distorted cubane is elongated along the C_2 axis: the average metal–metal distance (2.715 Å) in the planes (H planes) perpendicular to the C_2 axis is shorter than that (2.848 Å) in the planes (V planes) parallel to the C_2 axis. The average angle (75.2°) of M–S–M in the H planes is much smaller than its counterpart in the V planes (79.1°). The fact that the cross angle of 82.0° between Mo–Fe and Fe–Fe bonds of the H planes is much smaller than 90° indicates twisting of the cubane core. In this distorted cubane, each face is nonplanar and any pair of the opposite edges of the cubane is not coplanar.

Table IV. Selected Bond Angles (deg) for $[MoFe_3S_4(Me_2dtc)_5]\cdot 2CH_2Cl_2$

M′-M-Fe	65.07 (6)	S(1)-Fe-S(1)′	103.2 (1)
M-M′-Fe	58.51 (6)	S(1)-Fe-S(2)	104.3 (2)
Fe-M-Fe	57.34 (8)	S(1)′-Fe-S(2)	94.4 (2)
M-Fe-M	56.37 (7)	S(1)-Fe-S(21)	107.0 (2)
M-Fe-Fe′	64.63 (7)	S(1)-Fe-S(22)	101.3 (3)
M-Fe′-Fe	58.14 (6)	S(1)′-Fe-S(21)	148.7 (2)
S(1)-M-S(2)	102.9 (2)	S(1)′-Fe-S(22)	91.2 (2)
S(1)-M-S(2)′	92.4 (2)	S(2)-Fe-S(21)	86.2 (2)
S(2)-M-S(2)′	106.0 (1)	S(2)-Fe-S(22)	151.7 (2)
S(1)-M-S(11)	85.6 (1)	S(21)-Fe-S(22)	74.9 (2)
S(1)-M-S(12)	88.3 (2)	M-S(1)-Fe	76.0 (2)
S(1)M-S(13)	165.5 (1)	M-S(1)-Fe′	82.4 (2)
S(2)-M-S(1)	159.1 (2)	Fe-S(1)-Fe′	76.5 (1)
S(2)-M-S(12)	90.2 (1)	M-S(2)-M′	73.9 (1)
S(2)-M-S(13)	89.4 (2)	M-S(2)-Fe	76.0 (1)
S(2)′-M-S(11)	92.6 (1)	M-S(2)Fe′	81.8 (2)
S(2)′-M-S(12)	163.2 (1)	M-S(11)-C(10)	87.5 (4)
S(2)′-M-S(13)	91.7 (2)	M-S(12)-C(10)	88.5 (4)
S(11)-M-S(12)	70.8 (1)	Fe-S(21)-C(20)	89.1 (5)
S(11)-M-S(13)	80.4 (1)	Fe-S(22)-C(20)	87.7 (6)
S(12)-M-S(13)	83.8 (2)	M-S(13)-C(30)	112.8 (7)

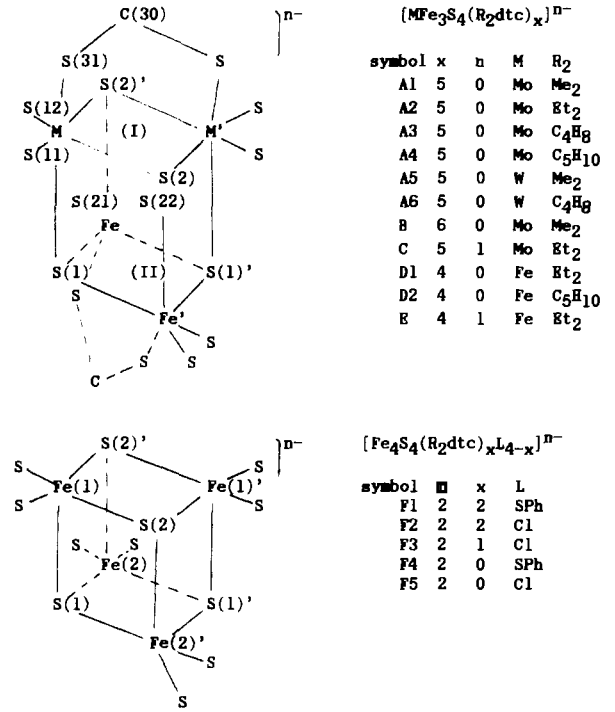

Figure 3. Atomic numbering system and symbol designation for single-cubane anions.

The $MoFe_3S_4$ core can be considered to consist of upper plane I, $[MoS_2Fe]$ with FeS_6 and MoS_6 moieties, and lower plane II, $[FeS_2Fe]$ with two identical S_3FeS_2 moieties (see Figure 3). A 2-fold disorder involving the FeS_6 and MoS_6 moieties of the core is applied to solve the structure (vide supra). This disordering phenomenon is possible from geometrical and energetical points of view and has been observed in other cases such as in the complex $(Et_4N)[Cl_2FeS_2MoS_2]$.[23] Therefore, the unique "cubane" $[MoFe_3S_4]$, oriented in the same way and repeated regularly and infinitely in crystal space, may be arranged randomly in a particular direction (Mo → Fe or Fe → Mo), so that the two moieties

(23) Tieckelmann, R. H.; Silvis, H. C.; Kent, T. A.; Huynh, B. H.; Waszczak, J. V.; Teo, Boon-Keng; Averill, B. A. *J. Am. Chem. Soc.* **1980**, *102*, 5550.

Table V. Angles (deg) between Direction Vectors of C–N Bonds in R_2dtc Ligands with a Single Cubane[a]

angle no.	bond 1	bond 2	angle A[b]	B	C	D2	E
1	N(3)–C(30)	C(10)–N(1)	89 (6)	87	76		
2	N(3)–C(30)	C(20)–N(2)	130 (4)	93	128		
3	N(1)–C(10)	C(10)′–N(1)′	174 (3)	173	152	97	120
4	N(1)–C(10)	C(20)–N(2)	91 (12)	90	98		104
5	N(2)–C(20)	C(20)′–N(2)′	99 (5)	174	104	88	120

[a] Atomic numbering according to Figure 2. [b] Average value of A1, A2, A3, and A4, with standard deviation in parnetheses.

Table VI. Comparison of Structural Parameters of Single-Cubane Clusters $[MFe_3S_4(R_2dtc)_x]^{n-}$[a]

	A[e]	B	C	D2	E
M–M′[c]	2.694 (9)	2.735	2.624	2.748	3.070
M–Fe[c]	2.859 (10)	2.870	2.868	2.728	2.845
Fe–Fe′	2.706 (18)		2.736		
M–S(2)	2.243 (5)	2.222	2.242		
M–S(1)	2.262 (5)	2.245	2.328		
Fe–S(1)	2.207 (8)		2.248	2.232	2.310
Fe–S(2)	2.239 (5)		2.326	2.248	2.248
M–S_t[d]	2.463 (6)	2.429	2.468		
Fe–S_t	2.308 (7)		2.524	2.283	2.397
S_t–Fe–S_t	74.9 (2)	76.1	69.6	76.1	71.7

[a] Symbol designations are listed in Figure 3. [b] Atomic distances (Å) or bond angles (deg). [c] M stands for Mo (W) or Fe in plane I, and Fe stands for the Fe or Fe′ in plane II as shown in Figure 3. [d] S_t stands for the S atom in R_2dtc. [e] Average value and standard deviation (parentheses) for A1, A2, A3, and A4.

$[FeS_6]$ and $[MoS_6]$ are interchangeable in that direction.

There are three types of R_2dtc ligands in this single-cubane cluster: (a) one bridged between two metal atoms (Mo and Fe); (b) two chelated individually to either Fe or Mo, which is six-coordinated in plane I; (c) the remaining two chelated individually to the two five-coordinate Fe atoms in plane II. If bond C–N is taken as the direction of the ligand, the angles between different ligands in various types of clusters are listed in Table V. In cluster A, B, or C, ligand a is parallel to the C_2 axis and nearly perpendicular to ligands b as shown by angle 1 in Table V, while ligands b in turn point directly at each other in plane I as indicated by angle 3 being close to 180°. The remaining two ligands tilt from plane II and form essentially a trigonal array with ligand a for clusters A and C but not for B, which possesses six R_2dtc ligands. The reduction, either from A to C or from D to E, induces a change of ligand direction as well as change of bond length (vide infra).

Comparison of Cubane Structures. The average atomic distances and bond angles of A type clusters $[MoFe_3S_4(R_2dtc)_5]$ with various ligands (A1, R = Me; A2, R = Et; A3, $R_2 = C_4H_8$; A4, $R_2 = C_5H_{10}$) are listed in Table VI along with data for other related single-cubane clusters. The crystal structures of $[MoFe_3S_4(R_2dtc)_5]^{0,-}$ (A1–A4, B, C) were best solved by the assumption of a 2-fold disorder.[6] Therefore, one can not distinguish atom Mo from atom Fe in plane I or Fe from Fe′ in plane II (see Figure 3), and the distance M–S is designated as the average atomic distances of Mo–S and Fe–S of plane I and the distance Fe–S as the average bond length of Fe–S and Fe′–S of plane II. The cubane is elongated along the pseudo-C_{2v} axis; viz., the order of bond lengths is M–S(1) > M–S(2) and Fe–S(2) > Fe–S(1) as shown in Table VI. This elongation is also confirmed by the fact that the atomic distance M–Fe is longer than M–M′ or Fe–Fe′ and their average values in compounds A are 2.86 Å vs 2.69 or 2.71 Å, in that order, and those in compound C are 2.87 vs 2.63 or 2.74 Å. This elongation is also present along the S_4 axis in compound B. Here the average bond length M–S(2) (2.222 Å) is shorter than M–S(1) (2.245 Å); and the average distance M–M′ (2.74 Å) is shorter than M–Fe (2.87 Å). The C_2 rotation symmetry and the elongation along this axis are similar to those in the cluster $[Fe_4S_4(SR)_4]^{3-}$,[1c] but not to those in compounds G or H–J where the cubane core is elongated along the 3-fold axis.[2-4]

Table VII. Isomer Shifts[a] (IS, mm/s) and Quadrupole Splittings (QS, mm/s) of $Fe(R_2dtc)$ in Cubane Clusters and Related Compounds

compound	298 K IS	298 K QS	80 K IS	80 K QS	no. of subsites
$Fe(Me_2dtc)_3$[b]	0.41	0.26	0.43	0.47	
$Fe(Et_2dtc)_3$	0.39	0.29	0.47	0.55	
$Fe(C_4H_8dtc)_3$[b]	0.40	0.36	0.51	0.42	
$[Fe_4S_4(SPh)_2(Et_2dtc)_2]^{2-}$[c] (F1)			0.64	1.84	
$[Fe_4S_4(Et_2dtc)_4]$ (D1)	0.34	1.03	0.41	1.42	
$[MoFe_3S_4(Et_2dtc)_5]$ (A2)	0.31	1.21	0.37	1.36	2
	0.29	0.34	0.36	0.28	1
$[MoFe_3S_4(Me_2dtc)_5]$ (A1)	0.32	1.32	0.36	1.36	2
	0.32	0.20	0.35	0.19	1
$[WFe_3F_4(Me_2dtc)_5]$ (A5)	0.34	1.23	0.40	1.30	2
	0.33	0.30	0.39	0.21	1
$[MoFe_3S_4(C_4H_8dtc)_5]$ (A3)	0.32	1.20	0.39	1.32	2
	0.31	0.31	0.38	0.33	1
$[WFe_3S_4(C_4H_8dtc)_5]$ (A6)	0.34	1.18	0.39	1.27	2
	0.33	0.40	0.39	0.34	1
$[MoFe_3S_4(Et_2dtc)_5]^-$ (C)	0.42	1.11	0.51	1.18	2
	0.43	0.88	0.54	0.86	1

[a] All isomers shifts are referenced to α-Fe metal at room temperature. [b] From ref 24. [c] From ref 8.

The extra electron of cluster C is delocalized among the metal atoms since the bond lengths Fe–S(1) (2.248 Å), Fe–S(2) (2.326 Å), and Fe–S_t (2.524 Å) in cluster C are longer than their counterparts in cluster A, being 2.207 (8), 2.239 (5), and 2.308 (7) Å, respectively. Although the atomic distances M–S(2) and M–S_t do not vary much from A to C, the effect of the extra electron on atom M is indicated by the lengthening of bond M–S(1) of C (from 2.262 to 2.328 Å).

Compression or elongation along the S_4 axis of the neutral cluster D2 is not obvious, but it is definitely compressed in the reduced cluster E. The atomic distance Fe–S_t in cluster D2 is approximately equivalent to the average value of that in cluster A, but differs very much from that in B, C, or E, as the oxidation state and the environment of Fe in cluster D2 are similar to those of A but different from those in the latter clusters.

The formal oxidation state of Fe in E is +2.75. The atomic distances Fe–S_c and Fe–S_t in E are longer than those in clusters A or D, but are nearly equal to those in C. On reduction, the extra electron moves among the three iron atoms instead of localized on one. This assumption is confirmed by Mössbauer data (vide infra).

Another important feature is the variation of chelating angle (bite angle) S_t–Fe–S_t′ of a single dialkyldithiocarbamato ligand with respect to the oxidation state of the Fe atom. The average oxidation state of Fe atom in plane II of cluster C, F1, or F2 is smaller than +2.75, and the average bite angle (69.7 (3)°) to the Fe atoms is slightly smaller than that in E (71.7°) where the average oxidation state of Fe is +2.75. In clusters A or D2, this angle (75.3 (5)°) is even larger, where the average oxidation state of Fe is +3.0. The ligand R_2dtc could exist in one of two resonance forms:

1 2

If Fe is an electron-deficient atom, e.g., in the high oxidation state +3, the ligand prefers form **2** with a shorter Fe–S_t bond and a larger S_t–Fe–S_t angle. Consequently, oxidation states of metal atoms in the same environment (i.e. the same type of metal atom, R_2dtc ligand, and coordination number) can be estimated from the atomic distances Fe–S_c and Fe–S_t and the bite angle S_t–Fe–S_t′.

Mössbauer Parameters. The Mössbauer parameters, obtained by least-squares fitting with the experimental absorption spectra, are shown in Table VII. The average isomer shift of ^{57}Fe in clusters $[MFe_3S_4(R_2dtc)_5]$ (M = Mo, W) at liquid-nitrogen temperature is 0.38 ± 0.03 mm/s, which is close to the value for Fe(III) in similar environment such as that in $[Fe_4S_4(Et_2dtc)_4]$

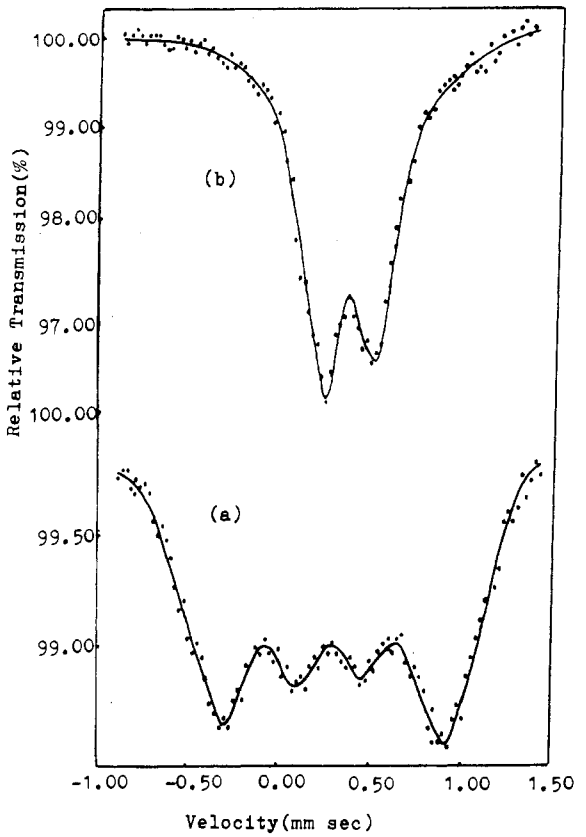

Figure 4. Mössbauer spectra at liquid-nitrogen temperature: (a) $[MoFe_3S_4(Et_2dtc)_5]$ (A2); (b) $(Et_4N)[MoFe_3S_4(Et_2dtc)_5]$ (C). Solid lines are the least-squares fits for the experimental data based on the parameters in Table VII.

or $[Fe(Et_2dtc)_3]$. There are two types of Fe atoms in cluster A with very distinct quadrupole splittings of 1.32 (3) and 0.27 (4) mm/s at liquid-nitrogen temperature. The former is similar to that of Fe(III) in $[Fe_4S_4(Et_2dtc)_4]$ (1.42 mm/s), where the Fe atom is five-coordinated, and the latter is close to the value in $[Fe(Et_2dtc)_3]$ (0.48 mm/s), where the Fe atom is six-coordinated. The absorption intensity ratio of the former to the latter is approximately 2:1. It is quite clear from these results that the valence state of Fe in clusters A is 3+ at either a five- or a six-coordinate center. The variations of alkyl substituents in R_2dtc and of metals (Mo or W) can not be distinguished from the data in Table VII.

In comparison with clusters A, cluster C possesses one more electron, which is not located at one particular Fe atom but is delocalized among metal atoms, as the isomer shifts of all three Fe atoms are changed. At liquid-nitrogen temperature, the isomer shift of 0.51 mm/s for S_3FeEt_2dtc in cluster C is less than that (0.64 mm/s) in $[Fe_4S_4(SPh)_2(Et_2dtc)_2]^{2-}$ where the oxidation level of the Fe atom is +2.5.[8] According to the argument that the isomer shifts of a series of Fe complexes containing well-defined Fe (mean) oxidation states (X) in similar sites should follow an empirical linear relationship, IS = $a - bX$, where a and b are constants.[24] Using the data X = 3.0, IS = 0.38 mm/s and X = 2.5, IS = 0.64 mm/s, we can deduce the mean oxidation state of Fe atoms in cluster C as X = 2.7 by interpolation of its IS value (0.53 mm/s). The Mössbauer spectra of A and C are depicted in parts a and b of Figure 4, respectively.

No significant change of IS or QS values of these samples between ambient and liquid-nitrogen temperatures is an indication that the energy difference between the ground state and the first excited state is much greater than the temperature range we are working at.

(24) Christou, G.; Mascharak, P. K.; Armstrong, W. H.; Papaefthymiou, G. C.; Frankel, R. B.; Holm, R. H. *J. Am. Chem. Soc.* **1982**, *104*, 2820.
(25) (a) Merrithew, P. B.; Rasmussen, P. G. *Inorg. Chem.* **1972**, *11*, 325. (b) Richards, R.; Johnson, C. E.; Hill, H. A. O. *J. Chem. Phys.* **1968**, *48*, 5231.

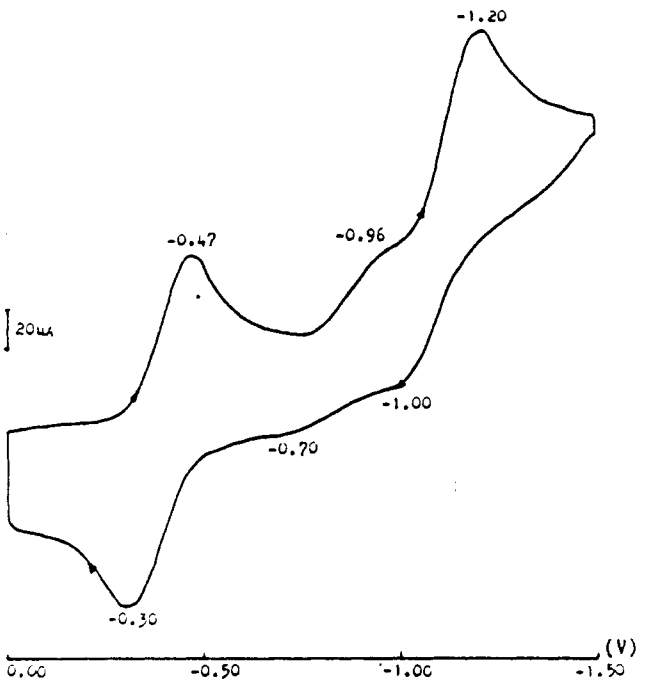

Figure 5. Cyclic voltammogram for $[MoFe_3S_4(Et_2dtc)_5]$ (A2, 0.002 M) in CH_2Cl_2 solution (0.1 M of Bu_4NBF_4, 100 mV/s).

Table VIII. Redox Potentials (V) of Clusters $[MFe_3S_4(R_2dtc)_5]$ (M = Mo, W) and Related Compounds in CH_2Cl_2 solution at Room Temperature

	0/1−			other redcns	
compound	$-E_{p,c}$	$-E_{p,a}$	$-E^a$	$-E_2$	$-E_3$
$Fe(Et_2dtc)_3$	0.56	0.28	0.42		
$[MoFe_3S_4(Et_2dtc)_5]$	0.47	0.30	0.39	0.96	1.20
$Fe(Me_2dtc)_3$	0.56	0.28	0.42		
$[MoFe_3S_4(Me_2dtc)_5]$	0.42	0.26	0.34	0.89	1.15
$[WFe_3S_4(Me_2dtc)_5]$	0.42	0.31	0.36	0.92	1.24
$Fe(C_4H_8dtc)_3$	0.47	0.32	0.40		
$[MoFe_3S_4(C_4H_8dtc)_5]$	0.41	0.23	0.32	0.96	1.20
$[WFe_3S_4(C_4H_8dtc)_5]$	0.46	0.22	0.34	0.96	1.34

$^a E = (E_{p,c} + E_{p,a})/2$.

Table IX. Proton Chemical Shifts (ppm) for the R_2dtc Ligands of $[MFe_3S_4(R_2dtc)_5]$ (M = Mo, W) and Related Compounds in DMSO-d_6 Solution at Room Temperature

	chem shift			
	R_2dtcFe		R_2dtcM	
compound	α-H^b	β-H^b	α-H^b	β-H^b
$Fe(Et_2dtc)_3$	50.1	1.2		
$Fe_4S_4(Et_2dtc)_4$	33.0	2.2		
$[MoFe_3S_4(Et_2dtc)_5]$	32.8	*c*	7.9	*c*
$Fe(Me_2dtc)_3$	67.1			
$[MoFe_3S_4(Me_2dtc)_5]$	45.7		9.4	
$[WFe_3S_4(Me_2dtc)_5]$	46.3		7.9	
$Fe(C_4H_8dtc)_3$[a]	89.1	6.5		
$[MoFe_3S_4(C_4H_8dtc)_5]$	39.5	2.1	4.7	2.1
$[WFe_3S_4(C_4H_8dtc)_5]$	41.2	*c*	5.0	*c*

[a] In a solution of Me_2CO-d_6. [b] α-H is the proton of $-CH_2-$ in Et or of $-CH_3$ in Me, and β-H is that of $-CH_3$ in Et. [c] Obscured.

Electrochemical Studies. Figure 5 displays the cyclic voltammogram of $[MoFe_3S_4(Et_2dtc)_5]$ in CH_2Cl_2. Redox and half-wave potentials of clusters A along with those of $[Fe(R_2dtc)_3]$ were tabulated in Table VIII. The potentials of the first redox couple are very similar for cluster compounds A even with different M or R and are slightly less negative than that in the monometal complexes $Fe(R_2dtc)_3$. This fact indicates that the first redox couple $[A]^0 \leftrightarrow [A]^-$ is a process of $Fe^{3+} \leftrightarrow Fe^{2+}$, and there is no significant contribution from the orbitals of Mo (or W). The extra electron in $[A]^-$ moves among different metal atoms as indicated

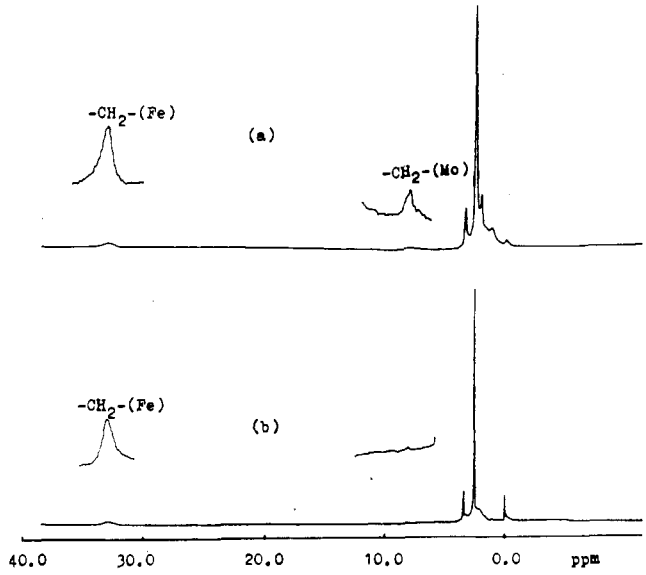

Figure 6. ^{1}H NMR spectra in DMSO-d_6 solution at room temperature: (a) $[MoFe_3S_4(Et_2dtc)_5]$ (A2); (b) $[Fe_4S_4(Et_2dtc)_4]$ (E).

by crystallographic and Mössbauer data (vide supra), and strong interaction of the metal atoms is inferred. The second and the third reduction potentials shift to more negative values. The average value of the third reduction potentials of the Mo complexes (−1.18 ± 0.03 V) is close to that (−1.19 V) of $[MoFe_3S_4(SPh)_3(R_2cat)]^{2-}$,[5c] and is different from that of the W analogues (−1.29 ± 0.05 V). The first redox couple is chemically reversible, but the second and the third are not.

^{1}H NMR Chemical Shifts. ^{1}H NMR spectra of clusters A2 and E containing the Et_2dtc ligand are depicted in Figure 6. There is only one type of ethyl group in cluster E, i.e. $-CH_2CH_3$ in the same environment of $S_3Fe^{III}(Et_2dtc)$. Thus it is reasonable to assign the absorption at 33 ppm to the proton of $-CH_2-$ and that at 2.2 ppm to the proton of $-CH_3$ in Figure 6b. It is interesting to note that the spectrum for A2 is relatively simple with a broad peak centered at 33 ppm. We believe that the Fe–S_t bond of the bridging ligand in cluster A2 may have cleaved in DMSO solution in the following manner:

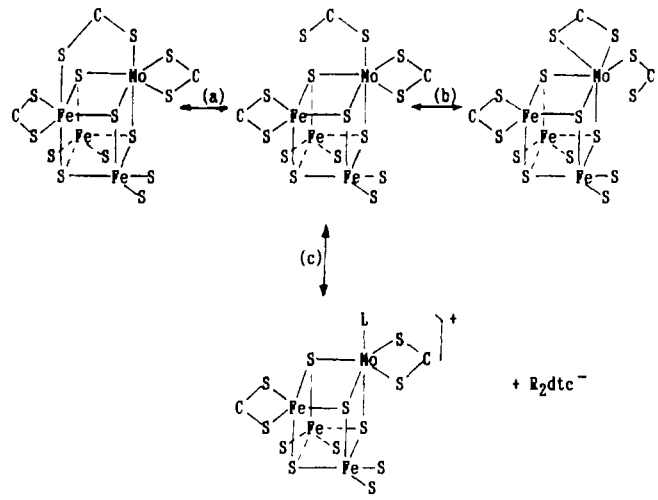

Consequently, there should be three types of R_2dtc in a DMSO solution of A2: (1) S_3FeR_2dtc, (2) R_2dtc attached to Mo as in $S_3Mo(R_2dtc)$, and (3) R_2dtc detached as in the anion R_2dtc^-. As the resonance of the methyl group is partially obscured by the absorption peaks of solvent and impurity, it is better to evaluate the absorption of the methylene protons. The absorption at 33 ppm for A2 is similar to that for E and it can be assigned to the methylene protons in a type 1 ligand. The resonance of methylene in a type 2 ligand is a broad peak at 8 ppm for A2. The facts that the intensity ratio between absorptions at 33 ppm and near 8 ppm is larger than 3:2 and that the spectrum structure in the region 1.2–4.0 ppm of A2 is more complicated than that of E are strong indications of solvent substitution (L) and production of free ligand (type 3). Palermo and Holm showed that solvent substitution occurs in the single-cubane cluster with thiophenol ligand.[5f,g] The proton chemical shifts of the R_2dtc ligands in various cubane clusters and iron complexes are listed in Table IX. It is clear that the signals of $[MoFe_3S_4(R_2dtc)_5]$ at low field do not differ much from those of the W compounds. The chemical shifts of the clusters are solvent dependent and may differ as much as 15 ppm in our experiments (not shown).

It is evident that clusters $[MFe_3S_4(R_2dtc)_5]$ are stable if all Fe atoms are in valence state 3+, which is indicated by the following facts: (i) most of the clusters reported in this work are in the form of A where all atoms Fe are in 3+ state; (ii) the first redox couple of A is that for $Fe^{3+} \leftrightarrow Fe^{2+}$; (iii) the valence electrons of Fe^{3+} form a stable half-filled shell and are relatively localized on the Fe atom. The isotropic shift is a combination of the dipole and contact shifts in the form:

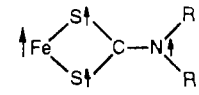

The dipolar mechanism depends on the magnetic moment of Fe and the geometry of the protons in respect to the magnetic center Fe. The contact mechanism relies very much on the delocalization of the unpaired electron, which in turn depends on the nature of the Fe atom and the basicity of the solvent that surrounds the N atom. This mechanism enables us to interpret the following experimental facts: (i) the R group is very far from the paramagnetic center of metal atom, yet the isotropic shifts of its protons are still sizable; (ii) the variation of solvents affects greatly the chemical shifts of the protons in the R group.

Conclusion

1. Single-cubane clusters with the $[MoFe_3S_4]$ unit can be obtained by a one-pot reaction with the bidentate ligand R_2dtc. It can also be synthesized through the linear intermediate $Fe(DMF)_6[(FeCl_2)_2MoS_4]$. The coordination nature of the bidentate R_2dtc is responsible for the formation of single-cubane clusters in spontaneous self-assembly processes.

2. Three more oxidation levels, 4+ (C), 5+ (A), and 6+ (B), are observed for the $[MoFe_3S_4]$ core in addition to the reported 3+ and 2+ states.[5] The resonance structure and low reduction ability of R_2dtc favor the formation of high oxidation levels of the core, and the most stable and commonly occurred product with the R_2dtc ligand is A with $[MoFe_3S_4]^{5+}$.

3. Clusters A and C contain a 2-fold or pseudo-2-fold axis passing through the bridging ligand linking atoms Fe and Mo. There is a 2-fold disorder involving the FeS_6 and MoS_6 moieties in the crystal arrangement.

4. All iron atoms in A are in oxidation state 3+ and each Fe atom exists in the localized d^5 electronic state, which is not greatly influenced by the orbitals of the neighboring metal atoms. However, the reduced form C possesses a highly delocalized electron.

5. In polar solvent, all Fe atoms in clusters A are in five-coordinate centers, so that there are only two types of R_2dtc ligands: one chelated to Fe and the other chelated to Mo. The latter is in an equilibrium of two forms: monodentate and bidentate. However, partial substitution by a solvent molecule is not excluded.

Acknowledgment. This work was supported by the National Natural Science Foundation and the Fujian Science Foundation. We thank Mr. Zhi Guo and Fang Wang for assistance with the Mössbauer data. Part of the NMR data was obtained at the Laboratory of Magnetic Resonance and Atomic and Molecular Physics (Wuhan). We are grateful to the reviewers for their critical comments on the paper.

Supplementary Material Available: Tables of anisotropic thermal parameters, crystallographic data, and bond angles (3 pages); a listing of calculated and observed structure factors (4 pages). Ordering information is given on any current masthead page.